35th Annual International Conference of the IEEE EMBS
Osaka, Japan, 3 - 7 July, 2013

Theoretical Study of Evaluation Method for MRI Metal Artifact

Yohei Sasaki, Masatake Akutagawa, Takahiro Emoto, Yoshinori Tegawa, and Yosuke Kinouchi

Abstract*— In dental field, the effect of the Magnetic Resonance Imaging (MRI) artifact generated by the magnetic metal is a significant problem. The MRI metal artifact occurs when using magnetic attachment and the keeper of the ferromagnetic substance remains implanted in the mouth as the MR image is taken. In this study, we theoretically evaluated and analyzed the artifact of MR images caused by the keeper based on the actual principle of MRI by means of simulation. As a result we were able to recognize the changes and distortion in the signal strength of the output image. We found that our results of output images and previously reported results of actual measurement are very similar. MRI artifact caused by dental magnetic metal showed that it can be reported by theoretical simulation.

I. Introduction

With the evolution of the MRI technology, MRI has become increasingly important in health care. On the other hand, many problems of artifacts by magnetic metal in the body have been reported [1] [2]. For example, about denture or knee prosthesis. In the dental field, several magnetic metals are used, such as inlay-crowns, bridges and implants, among which, is the magnetic attachment. [3] [4]. The magnetic attachment is a denture that uses magnets. It requires no metal parts such as clasps, hence with superior aesthetic and can be used as abutment tooth for poorly conditioned teeth. In addition, since handling is simple, it is suitable for the elderly as well. Different from the mechanical dentures, it has many new features which make it possible to maintain effective dental prosthesis with excellent clinical reputation. Generally, the magnetic attachment consists of the keeper that is implanted into the oral cavity and the magnet structure that is embedded in the denture. The attractive force between the keeper and the magnet structure of the magnetic attachment is used to retain the denture [5] [6]. The keeper is made of magnetic stainless steel. Though, it has a large burden on the patient because it is embedded in the oral cavity and is difficult to remove.

MRI is a tool that is able to image the body without being exposed to radiation. However, its principle is very complex. The magnetic field inside the MRI equipment is controlled by static magnetic field and gradient magnetic fields .So MRI can attach an image to the correct coordinate. If the keeper of the magnetic attachment left in the mouth, it becomes magnetized and behaves like a magnet in MRI. As a result, the magnetic field is disturbed. This is the cause of the artifact [7]. Some cases of artifacts effects in images by actual measured has been reported in previous studies [8] [9]. In fact, artifacts depend on specifications of MRI, material and shape of the keeper [10] [11] [12]. But, it is considered to be difficult to obtain range of artifacts from measured image. In this paper, we investigate the impact on the MR image caused by keeper, and analyze image based on the principle of MRI, and then compare the output image with previous studies through simulation. Results of the simulation showed a similar image as shown in the previous studies. The main purpose of this study is to theoretically elucidate and evaluate the cause of the MRI metal artifacts.

Corresponding author, Y. Sasaki is with Graduate School of Advanced Technology and Science, The University of Tokushima. 2-1 Minamijyosan-jima-cho, Tokushima, 770-8506, JPN. (corresponding author to provide e-mail: y-sasaki@ee.tokushima-u.ac.jp). M. Akutagawa, Takahiro Emoto, and Yosuke Kinouchi are with Institute of Technology and Science, The University of Tokushima.2-1 Minamijyosanjima-cho, Tokushima, 770-8506, JPN. (e-mail: makutaga@ee.tokushima-u.ac.jp). Y. Tegawa was with Institute of Health Biosciences, University of Tokushima.

II. Method

A. Principle of NMR

The MRI is imaged using a nuclear magnetic resonance phenomenon (NMR) to make proton of the body be resonant using a magnetic field. MRI equipment apply static magnetic field to the proton of the body, and the proton reaches the low energy state. When RF-pulse is radiated in the area, Proton in imaging area would be at a high-energy state. This frequency is called as the Larmor frequency. RF-pulse has same frequency as Larmor frequency. Then the high-energy proton upon releasing energy, receives FID-signal which eventually creates an MRI image. γ is defined as NMR ratio of hydrogen atoms (42.58MHz/T), B is magnetic flux density, Larmor frequency is computed as

$$v = \frac{1}{2\pi}\gamma \cdot B \tag{1.1}$$

Larmor frequency is proportional to the magnetic flux density. We analyzed for magnetic flux density.

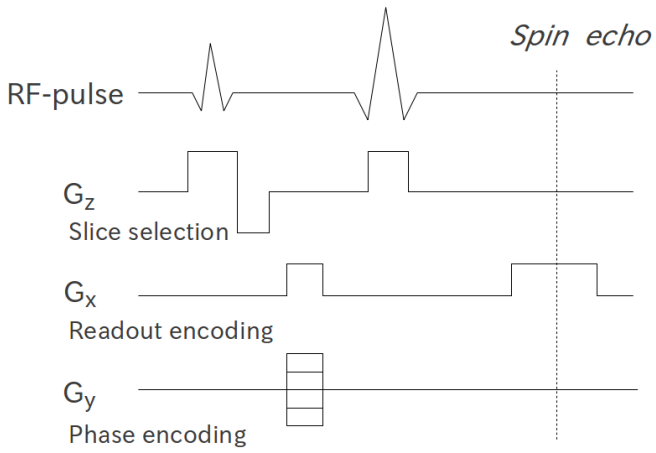

Figure 1. Spin echo imaging method. By performing slice selection, phase encoding and frequency encoding, the coordinates of the imaging area (x, y, z) is determined.

B. Imaging Sequence.

Amount of metal artifacts by the keeper is depending on the specification and performance of MRI. Especially, pulse sequence is one of the significant factors on the artifact. In this study, spin echo sequence (SE) are employed to reconstruction of the image. Imaging sequence use SE showed in (Fig. 1). Of these, slice selection and readout encoding are affected by disturbance of the magnetic field. We analyzed the slice selection and readout encoding.

C. Theory and the Imaging Conditions

P(x, y, z) denote actual coordinates of the imaging area, ρ(x, y, z) denote proton density at (x, y, z). There is non-uniform magnetic field, actual coordinates change to reconstructed coordinates as an image. P'(x', y', z') denote reconstructed coordinates as an image. In this paper, z coordinate change in the slice selection, x coordinate change in readout encoding. But the defined y coordinate does not change in phase encoding.

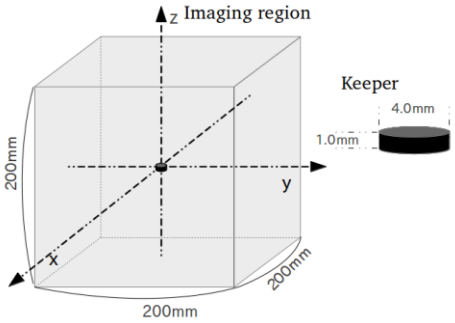

Figure 2. Imaging region and keeper. The origin coordinate is (0,0,0).Gradient magnetic field is applied along the axis.

The imaging region is a square cubic (200mm × 200mm × 200mm). Keeper is a disk-shaped, height of (1.0mm), diameter of (4.0mm), of a ferromagnetic substance such as SUS403. It is located in the center of the imaging region. In (Fig. 2) of the imaging region, there are magnetic field, static magnetic field "B_0", gradient magnetic field "$G(r)$", and keeper's magnetic field "$B_{dp}(r)$."Keeper's magnetic field is computed using the theoretical formula of the magnetic dipole. r denote distance of P from keeper. Three magnetic fields are computed as

$$B_0 = \begin{pmatrix} 0 \\ 0 \\ B_0 \end{pmatrix} \tag{2.1}$$

$$G(r) = \begin{pmatrix} 0 \\ 0 \\ G_x x + G_y y + G_z z \end{pmatrix} \tag{2.2}$$

$$B_{dp}(r) = \begin{pmatrix} \dfrac{3zx}{r^5} \\ \dfrac{3zy}{r^5} \\ \dfrac{3z^2}{r^5} - \dfrac{1}{r^3} \end{pmatrix} = \begin{pmatrix} B_{dpx} \\ B_{dpy} \\ B_{dpz} \end{pmatrix} \tag{2.3}$$

In this case, static magnetic field B_0 (1.5T), gradient magnetic field $G_x : G_y : G_Z$ (10 mT/m), Dipole moment m is computed as $V \times J$ Where, V is the volume of the keeper. J is used of magnetic field (1.5T). However, Keeper's magnetic flux density is not simply proportional to the external magnetic field. m is expected to be lower than this case in actual MR imaging.

D. Slice Selection

Slice selection is the operation of determining the coordinates of z. RF-pulse frequency is equal to the Larmor frequency. When MRI equipment irradiates the RF-pulse, protons of area equal to the Larmor frequency will be resonated. The resonance region is recognized as z coordinate. Magnetic flux density of P computed as

$$B(r) = \begin{pmatrix} 0 \\ 0 \\ B_0 \end{pmatrix} + \begin{pmatrix} 0 \\ 0 \\ G_z z \end{pmatrix} + \begin{pmatrix} B_{dpx} \\ B_{dpy} \\ B_{dpz} \end{pmatrix} \tag{2.4}$$

If the keeper does not exist, the two present magnetic fields are gradient magnetic field and static magnetic field. But, considering the magnetic field caused by the keeper, the relationship between actual coordinate z and reconstruction coordinate z' computed as

$$B_0 + G_z z' = \sqrt{B_{dpx}{}^2 + B_{dpy}{}^2 + \left(B_0 + G_z z + B_{dpz}\right)^2} \tag{2.5}$$

z' computed as

$$z' = \frac{\sqrt{B_{dpx}{}^2 + B_{dpy}{}^2 + \left(B_0 + G_z z + B_{dpz}\right)^2} - B_0}{G_Z} \tag{2.6}$$

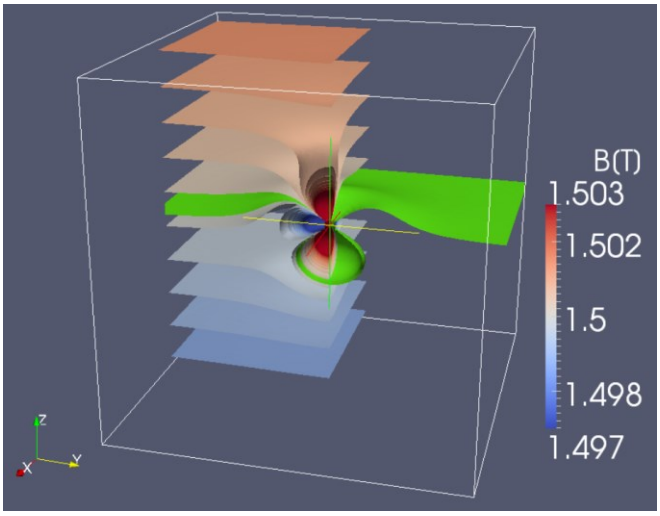

Figure 3. Resonance region in slice selection. The green region shows magnetic flux density of (1.500T ± 50 μT). The resonance region is highly distorted near the keeper.

A geometric distortion occurred from the relationship between z' and z which was analyzed using equation (2.6) In (Fig. 3). We found that z 'and z have greater difference near the keeper. By this geometric distortion, signal strength of the image changes after reconstruction. The change in signal the

enhanced image of T1-weighted (where high proton density is white, low proton density is black). However, the signal strength changes in the image of metal artifacts, shows low strength at black region as well as white regions in the image as shown in (Fig. 4). Width *dz'* of the reconstructed position z' is compared to width *dz* of the original position z. There is a difference in the width of *dz*. When *dz* is narrow, the signal strength is lower than actual image (black region), and when *dz* is wide, the signal strength is higher than actual image (white region).

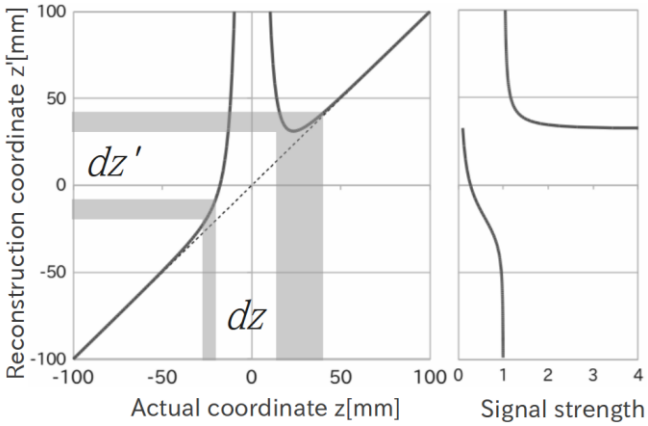

Figure 4. Imaging region and keeper. The origin coordinate is (0,0,0). Gradient magnetic field is applied along the axis.

E. Phase encoding and Readout encoding

When the resonated proton in the slice selection releases energy, a signal is called Free Induction Decay (FID) signal. The FID signal, frequency and phase are different in each coordinate. By receiving this signal, image is created by means of inverse Fourier transform. First, we discuss about the phase encoding. Before receiving the signal, there is a certain time when gradient magnetic field is applied to the y-axis, and eventually stopped. Because of this action, the phase along y-axis is shifted. However, strain y-axis direction will not occur [13]. Relationship between actual coordinate and y coordinates and after reconstruction y' is computed as

$$y' = y \tag{2.7}$$

Readout encoding is performed upon receiving FID signal after phase encoding. Because of application of gradient magnetic field along x-axis, there is shift in frequency along x-axis. FID signal frequency is proportional to the magnetic flux density in the region. Magnetic flux density of P computed as

$$B(r) = \begin{pmatrix} 0 \\ 0 \\ B_0 \end{pmatrix} + \begin{pmatrix} 0 \\ 0 \\ G_x x \end{pmatrix} + \begin{pmatrix} B_{dpx} \\ B_{dpy} \\ B_{dpz} \end{pmatrix} \tag{2.8}$$

Relationship between actual coordinate and x coordinates and after reconstruction x' is computed as

$$B_0 + G_x x' = \sqrt{B_{dpx}{}^2 + B_{dpy}{}^2 + \left(B_0 + G_x x + B_{dpz}\right)^2} \tag{2.9}$$

x' computed as

$$x' = \frac{\sqrt{B_{dpx}{}^2 + B_{dpy}{}^2 + \left(B_0 + G_x x + B_{dpz}\right)^2} - B_0}{G_x} \tag{2.10}$$

III. RESULT

We simulated artifact images for (2.6), (2.7) and (2.10).

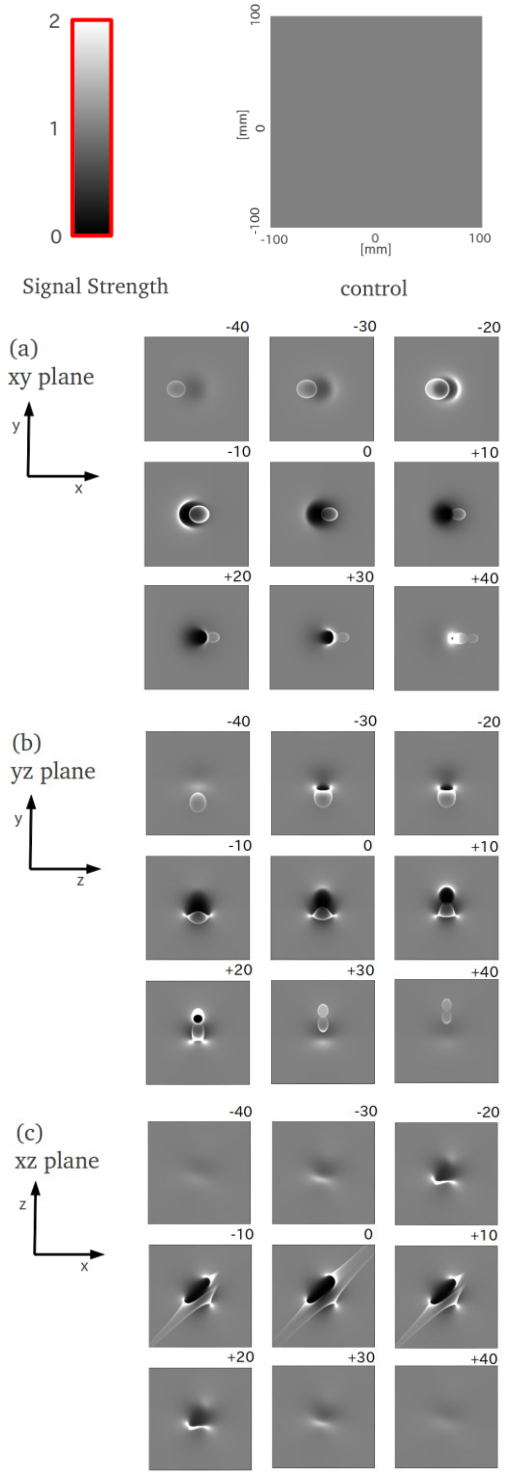

Figure 5. Output images. xy plane (a), yz plane (b), xz plane (c). These images were output at 201 × 201 [pixel] as 1[mm] is 1[pixel]. The number above the images denote distance from keeper.

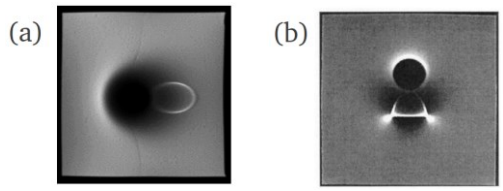

Figure 6. Measured images. (a) [7], (b) [14]. The area of (a) is xy plane of 150[mm] cubic phantom. This cubic phantom is filled with ager-ager, and used by 1.5[T] MRI. The area of (b) is yz plane of 200[mm] cubic phantom. This cubic phantom is filled pure water, ager and salt, and used by 3.0[T] MRI.

Fig. 5 (a) shows xy plane image (axial). Here, the signal level is reduced at the center of the images. In addition, there is also a characteristic white circle at the center of image. This is as a result of excitation at z position of another slice plane at the time of slice selection. Image at a distance z: 0 [mm] from the keeper is very similar to the existing results in Fig. 6 (a). Fig. 5 (b) shows yz plane image (sagittal). We can clearly tell that both this image and the control image are greatly distorted. Image at a distance x: +10 [mm] from the keeper is very similar to the existing result in Fig. 6 (b). Fig. 5(c) shows xz plane image (coronal). We found that the image is more greatly distorted compared to other slice planes. However, the artifact gets relatively smaller as it moves away from the keeper. At high signal strength regions, there is high concentration of reconstruction coordinates. When original coordinates are mapped in the same coordinates after reconstruction, the addition of signal is carried out and eventually the density increases as the well as the signal strength. Conversely when the signal is low, it is showed in black in the image and after reconstruction the density of the coordinates becomes low. With such image, where there is a significant degree of change in signal strength, it is difficult to use in the medical field for diagnosis because of the great distortion from the original image. However, where there is little change from the original state of the image, diagnostic imaging is considered quiet possible.

IV. Discusion and Conclusion

In this study, our analysis was based on the principle of the actual MRI. We theoretically evaluated the cause of the artifacts. It is evident that the prediction of the artifact is possible since we showed a similar tendency to previously reported results. Currently, Range of artifacts is determined from the image that has been captured by the measurement. However, there is an advantage with the simulation where a range of artifact is possible, if we know specifications of MRI, material and shape of the keeper. Recently, there have been discussions about proposed indicators on how to reduce the artifact of MRI. [15] [16]. This study based on theory can be of contribution to the reduction of the artifact.

Usually patients using magnetic attachment must remove the keeper when taking MRI. However, if there is no effect on the imaging region, there is no need to remove the keeper. It is necessary to indicate the artifact impact on MR images basing on the shape and material of the keeper. This study is based on the theory, it is effective to determine the area of the artifact.

Acknowledgment

Authors would like to acknowledge Professor Shinsuke Konaka of Institute of Technology and Science, The University of Tokushima for his advice during the weekly study meetings they had. Not forgetting, authors also appreciate Kaliba Aggrey of Graduate school of Advanced Technology and Science, University of Tokushima for his advice on Magnetic Attachments.

References

[1] M. H. Bagheri, M. M. Hosseini, M. J. Emami, and A. A. Foroughi, "Metallic artifact in MRI after removal of orthopedic implants," *European Journal of Radiology*, vol. 81, Mar. 2012, pp. 584-590.

[2] T. J. Heyse, J. Figiel, U. Hähnlein, N. Timmesfeld, J. Schmitt, M. D. Schofer, S. F-Winkelmann, T. Efe, "MRI after unicondylar knee arthroplasty : The preserved compartments," *The Knee*, vol. 19, Dec. 2012, pp. 923–926.

[3] Gillings BR. "Magnetic retention for complete and partial overdentures. Part I," *The Journal of Prosthetic Dentistry*, vol. 45. 1981, pp. 484-491.

[4] Gillings BR. "Magnetic retention for overdentures. Part II," The *Journal of Prosthetic Dentistry*, vol. 49, 1983. pp. 607-618.

[5] O. Okuno, S. Ishikawa, FT. Imuro, Y. Kinouchi, H. Yamada, T. Nakano, H. Hamanaka, N. Ishihata, H. Mizutani, and M. Ai, "Development of Sealed Cup Ypke Type Dental Magnetic Attachment," *Dental Materials Journal*, vol. 10, no. 2, 1991, pp. 172-174.

[6] Y. Suminaga, F. Tsuchida, N. Norio, T. Hosio, K. Sugiyama, "Surface Analysis of Keepers on Dental Magnetic Attachments: Comparison of Cast Bonding Technique and Direct-Bonding Technique," *Prosthodontic Research and Practice*, vol.3, no. 1, 2004, pp. 62-68.

[7] D. Destine, H. Mizutani, Y. Igarashi, "Metallic Artifacts in MRI Caused by Dental Alloys and Magnetic Keeper," *Jpn Prosthodont Soc*, vol.52, 2008, pp. 205-210.

[8] A. L. F. Costa, S Appenzeller, CL. Yasuda, F. R. Pereira, V. A. Zanardi, F. Cendes, "Artifacts in brain magnetic resonance imaging due to metallic dental objects" *Med Oral Patol Oral Cir Bucal*. 2009 Jun 1;14(6):E278-82.

[9] F. Shafiei, E. Honda, H. Takahashi, and T. Sasaki, "Artifacts from Dental Casting Alloys in Magnetic Resonance Imaging" *Journal of Dental Research* 82(8):602-606, 2003.

[10] FT .Iimuro, "Magnetic resonance imaging artifacts and the magnetic attachment system" *Dental Materials Journal*, 1994, 13, pp. 76-88.

[11] J. Starcukova, Z. S. Jr., H. Hubalkova, and I. Linetskiy, "Magnetic susceptibility and electrical conductivity of metallic dental materials and their impact on MR imaging artifacts" *Dental Materials*, vol.24 2008, pp. 715–723.

[12] T. Taniyama, T. Sohmura, T. Etoh2, M Aoki, Eiji Sugiyama, and J. Takahashi, "Metal artifacts in MRI from non-magnetic dental alloy and its FEM analysis" *Dental Materials Journal*, 2010; 29(3): 297–302.

[13] W. Lu, K. B. Pauly, G. E. Gold, J. M. Pauly, and B. A. Hargreaves, "SEMAC: Slice Encoding for Metal Artifact Correction in MRI Magnetic Resonance in Medicine" *Magnetic Resonance in Medicine* 62: 2009, pp. 66–76.

[14] The Japanese Society of Magnetic Applications in Dentistry Magnetic Attachment and MRI: Dental magnetic attachment user's MRI Safety Standards Manual, 2012.

[15] P. RCabrera, J.P.M. Duynhovenb, A. V. Toorna, and K. Nicolay, "MRI of hip prostheses using single-point methods: in vitro studies towards the artifact-free imaging of individuals with metal implants" *Magnetic Resonance Imaging* 22 (2004): pp. 1097–1103.

[16] W. Lu, K. B. Pauly, G. E. Gold, J. M. Pauly, and B. A. Hargreaves, "Slice Encoding for Metal Artifact Correction With Noise Reduction" *Magn Reson Med*. 2009 July; 62(1): pp. 66–76.